

# CAD IN AERODYNAMIC AIRCRAFT DESIGN

A. Ronzheimer,  
DLR, Institute of Aerodynamics and Flow Technology, Braunschweig, Germany

## Abstract

Computational fluid dynamics (CFD) has become a state of the art analysis tool for nearly all phases of aircraft design. In contrast to CFD, computer aided design (CAD) is traditionally used in later design phases of an aircraft, when the design is almost frozen. However, with the appearance of parametric CAD systems a new design methodology was enabled, which was based on the capability of a parametric CAD system to replay construction sequences with varied design parameters. A parametric wing can be re-used to create a vertical tail plane or parts can be associated to other parts, which allow concurrent engineering practices. In the present study, these capabilities have been exploited to generate extremely variable aircraft CAD models ready for CFD. Furthermore, parametric construction strategies, which have been developed in the past, are applied to model the primary aircraft parts, such as wing, fuselage and nacelle and also secondary parts, such as the belly fairing, wing tips and pylon, with the CAD system CATIA V5. For the construction of curves, which are used to create surface lofts, primarily B-splines are utilized, where the coordinates of the control points can later be used as the design parameters. Finally, the capabilities of parametric CAD are demonstrated through design variations performed for conventional configurations and through design studies with non-conventional aircraft configurations, which are in the focus of current research.

## 1. INTRODUCTION

Computational Fluid Dynamics (CFD) has become an indispensable tool in aerodynamic aircraft design. While 25 years ago the calculation of the inviscid flow field around an aircraft configuration consisting only of wing, body and nacelle was a real challenge, [1], today viscous CFD simulations are performed routinely in nearly all design phases of an aircraft. Especially in late phases high fidelity CFD is used to simulate the flow at the corners of the flight envelope in cruise flight and also for take-off and landing. When unstructured meshing and solver techniques, see [2], came up, the spectrum of applications using CFD was significantly enhanced. Currently there seems to be no limit regarding the geometrical complexity and the time to perform simulations for new aircraft configurations, as shown in FIGURE 1, has been reduced from months to days.

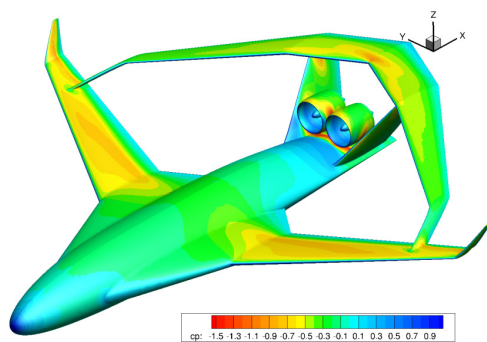


FIGURE 1. CFD for a novel aircraft configuration

Today, there is also an increasing demand from aircraft industry to use high fidelity CFD very early in preliminary and also in conceptual design phases. The reason is that CFD simulations can predict compressible and viscous flow fields around a given aircraft while accounting for all

relevant aerodynamic phenomena and deliver forces either on points on the surface or integral forces on any component. In the end these forces include viscous, transonic and also interference effects between components with a reliable accuracy. Especially in cases where these effects interact considerably, as is shown in FIGURE 2 for an aircraft configuration with under and over the wing mounted engines, the use of high fidelity CFD methods highly recommended.

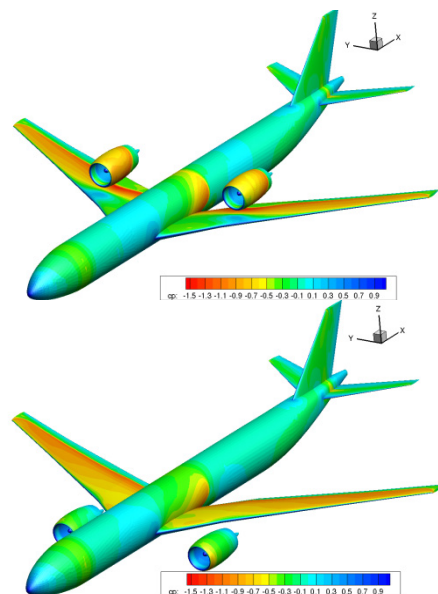


FIGURE 2. Comparison of CFD solutions for a transport aircraft configurations with over- and under-wing mounted nacelles

Moreover, if novel configurations are of interest an estimation of interference drag with traditional preliminary

design methods is difficult or even impossible, since these methods are predominantly tailored and calibrated for the design of ordinary aircraft concepts. Thus only high fidelity simulations can mitigate the risk of making wrong decisions in early design phases. This is particularly the case in a conceptual design phase when novel transport aircraft concepts are considered for alternative propulsion, which is currently in the focus of research.

However for a routine use of high fidelity CFD in early design phases, three major aspects have to be considered. The first aspect is the turnaround time, i.e. the time required to perform a complete cycle, including pre- and post-processing. Fortunately in the past decades great progress in computer technology was made towards massive parallel computer systems which led to a reduction of computer time from hours to minutes. Secondly the change from structured to unstructured methods has reduced the amount of time for grid generation significantly. Particularly the lack of automation for adapting or setting up the mesh blocking structure for a new configuration prevented routine and rapid grid generation in the past. Today unstructured methods are able to generate a grid around a clean geometry of medium complexity fully automatically in a couple of minutes. A third aspect, which is not directly seen in conjunction with CFD simulations, is the generation of a suitable geometry. This geometry should represent a feasible aircraft configuration and should be convenient for CFD simulations.

Today nearly all grid generation systems for high fidelity CFD simulations are demanding at first a watertight geometry. Furthermore the geometry has to be made available for the grid generation software either in the native format of the grid generator or in a neutral CAD format i.e. IGES or STEP. Water tightness of geometry can be established by clean intersections of components with each other. Experience has shown that this is best done with a commercial high end CAD system, if intersections are not already contained in the CAD data. As currently CFD simulations are predominantly conducted in late design phases, where a detailed CAD-model of the outer surface of the aircraft is already available, as shown in FIGURE 3, the transition from CAD to CFD grid generation is still the most critical process step, which requires more or less manual interactions for cleaning, de-featuring and setup of the geometry.

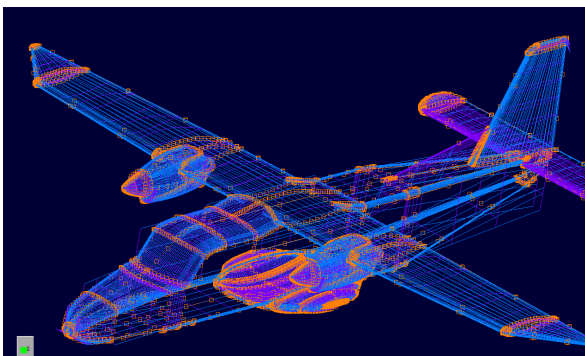


FIGURE 3. Geometry in boundary representation (b-rep) for mesh generation containing intersection curves

For the use of high fidelity CFD in early design phases an adequate geometry generator is a basic pre-requisite for the simulation chain and therefore, a certain effort was

spent to develop and exploit novel techniques, which also permit the use in multidisciplinary design optimizations environments, as described in [3]. At first the freeform deformation technique, which was proposed in [3], was applied to existing CAD data in the native format of the grid generator to generate new shapes through deformation. The method, described in [5], was later used to deform surface grids of the CFD mesh in shape optimization loops. However, in cases where only parts of a geometry are deformed, i.e. a wing, all affected intersection curves had to be re-calculated and updated. Finally, a high end parametric CAD system, namely CATIA V5 from Dassault Systemes, [6], was used as geometry generator for simulation based aircraft design. However, the utilization of CAD in early design phases is still doubtful since in classical textbooks, dealing with aircraft design, it is recommended to use CAD very late in the development cycle after the geometry is frozen. Furthermore, the problem arises that CFD engineers are usually not familiar with CAD systems and therefore, they expect specific and well-prepared geometries, which are ready for CFD meshing.

Fortunately, with the release of high end parametric CAD-systems from Parametric Technology [7], Dassault Systemes, and Siemens (formerly Unigraphics) [8], at the end of the last century a new design methodology was enabled. Due to the possibility to re-use a parametric design by simply changing design parameters, also non CAD-experts are enabled to utilize high end CAD to generate CAD-models for simulations or even for production. In contrast to conventional CAD systems, a parametric system has the outstanding property that in each construction step, i.e. the construction of a line, parameter values and names of the involved parent entities are stored. This is carried out automatically by the software, during interactive work with mouse and keyboard. If a parameter of a former construction step is changed, the construction of all affected child entities is repeated until all entities are up-to-date. This also can be performed in batch mode, which is an important prerequisite for design automation and design optimization.

Today, parametric CAD systems are widely used in virtual product design and are able to manage the complete lifecycle from preliminary design to disposal of a product. The objective of this study was to explore the capabilities of parametric CAD in early aerodynamic design of transport aircraft. In this phase of the design there is normally little knowledge about the shape of a new aircraft. At a basic level, the aircraft will have a fuselage to encase the payload, a wing to produce lift, a propulsion system to compensate the aerodynamic drag, and an empennage for stable flight. Depending on the concept, these parts are arranged in a certain way and are intersecting. The challenge is now to make all mentioned CAD-parts available and convenient for aerodynamic design.

## 2. PARAMETRIC MODELLING STRATEGY

When using a parametric CAD system the sequence of construction steps and their appropriate parameters, which are required to create a CAD part, are more important than the part itself. To achieve a high level of re-usability and variability of parametric CAD-parts it is obvious that a more advised and forward-looking modelling or construction strategy is required. In the

following sections the construction strategy is described for CATIA V5, but it should be possible to apply a similar procedure with any other high end parametric CAD-system.

Classically the primary function in aircraft geometric design for the modelling of surfaces is the loft-function, which can be found in CATIA in the generative shape design workbench, among other functions for the creation of curves and surfaces. A typical problem for using the loft function is shown in FIGURE 4, where a propeller blade is lofted.

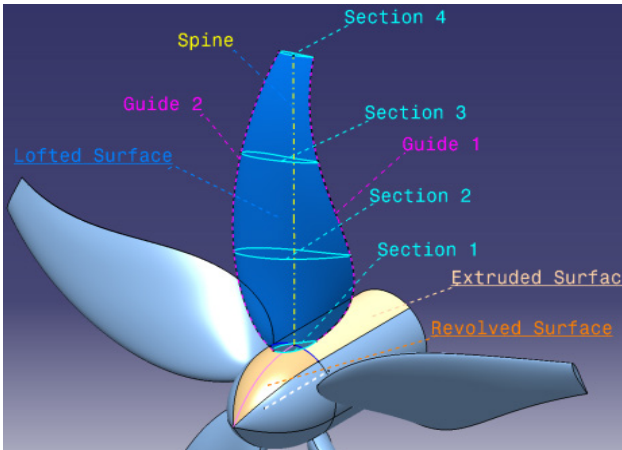


FIGURE 4. Surfaces created with revolve-, extrude- and loft-function in CATIA V5

The loft function requires ideally planar section curves and three-dimensional guiding curves, which connect the individual sections. In the case of a propeller the guiding curves lie on helical surfaces. Additionally a spine curve can be specified. In addition to the loft-function, which is used for about 90% of the outer surfaces of an aircraft, extrude-, revolve- and sweep function are available. In the case of the propeller, shown in FIGURE 4, the sweep-function is used to generate the helical surfaces. Practice showed that it is expedient to first construct a wireframe of curves before the surface creation with loft-, extrude-, revolve- or sweep functions is performed. However, in some cases exceptions have to be made, since for the construction of nose- and trailing edge curves of the propeller-example the helical surfaces are required as support surfaces for projections. It was also found, that it is more practical to first construct the guiding curves and to fit in the section curves afterwards, using transformation- and scaling-functions of the CAD-system.

### 3. WIREFRAME MODELLING

In case of an aircraft typically two different types of primary shapes exists: wing-type shapes and fuselage type shapes. In case of wing-type shapes the defining sections are parallel to the flow direction and are typically airfoils, while in case of fuselage-type shapes the defining sections are normal to the flow direction and are symmetrical. Examples of wireframe curves and corresponding surfaces of fuselage, wing and nacelle are shown in FIGURE 5, FIGURE 6 and FIGURE 7. In this study the engine consists of a through-flow nacelle and an internal body of revolution, which was added to achieve a realistic flow around the nacelle lip and in the inlet area. The essential construction work was the preparation of adequate section- and guiding-curves with the CAD

system. In general the construction work starts with the wireframes of the primary surfaces.

After the primary surfaces have been lofted and positioned, wireframes for secondary surfaces were created, since their wireframe curves depend on entities of the primary surfaces, which may result from intersections or projections and other operations. For example, for the wireframe of the pylon, see FIGURE 8, at first a curve is required, which results from the intersection of the wing surface with the nacelle symmetry plane. In case of a new position of the nacelle, the construction of the pylon is repeated and starts again with the plane/surface intersection. In FIGURE 9 a belly faring and in FIGURE 10 a wing tip is shown. In a similar way, further components as for example control surfaces or a high lift system may be added.

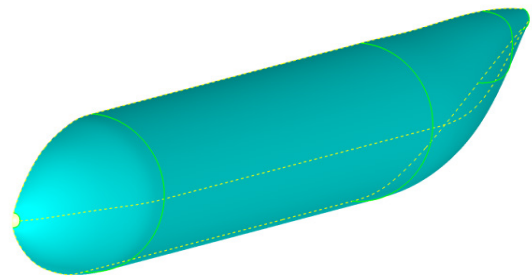


FIGURE 5. Parametric fuselage

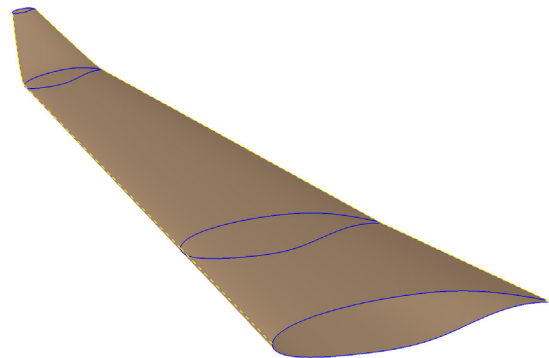


FIGURE 6. Parametric wing

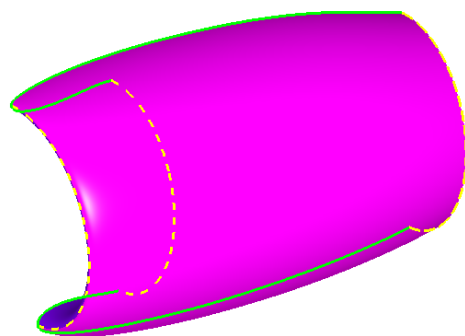


FIGURE 7. Parametric engine nacelle

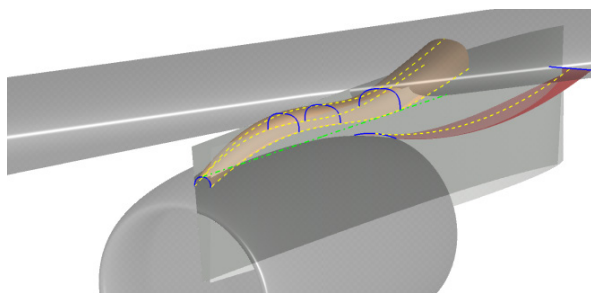


FIGURE 8. Pylon surfaces for underwing mounted engine

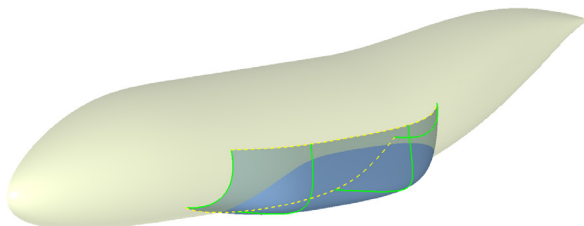


FIGURE 9. Belly fairing for low wing configuration

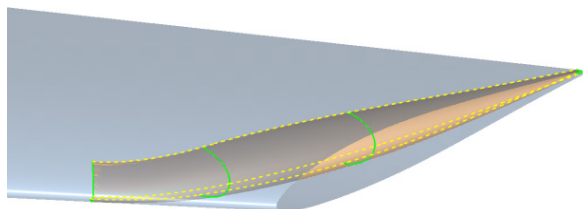


FIGURE 10. Wing tip surfaces

The belly fairing model, shown in FIGURE 9, was originally constructed within a former study, dealing with the DLR LAMAIR-configuration, [9], shown in FIGURE 11. Since this configuration has a forward swept wing, variations of the belly fairing shape were done to explore flow phenomena caused by the forward swept wing. For the present study the belly fairing construction was quite simply re-used.

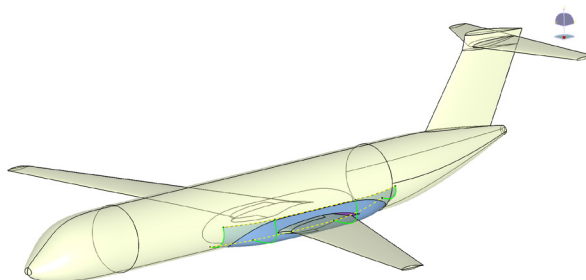


FIGURE 11. TULAM configuration with belly fairing

#### 4. PARAMETRIC CURVES

The variability of the aircraft surface representation is finally enabled either by the positioning of parts or via the defining curves forming the wireframe. The shape of a freeform curve in CAD is either determined directly with a parameter, i.e. the radius of a circle, or it is defined indirectly, as for example via coordinates of points, through which a spline-curve is fitted.

#### 4.1. Wing Sections

A spline fit curve is shown exemplarily in FIGURE 12 for a wing airfoil. In this example several problems with splines can be depicted. As can be seen a spline curve which fits the points tends to wiggle, which occurred obviously at the nose where curvature is high. To obtain a smooth curve in this special case, manual interaction and inspection is required to allow an approximation of the points. This however, is contrary to the automation of the curve generation. Also, if each single point-coordinate is variable, the number of design parameters would be unmanageably high in the case of several sections used for the loft surface. Besides this, it was observed that the CAD system requires a certain amount of time to process the spline-fit curves. It tries to find the smoothest NURBS-curve, see [10], which fits the points best with a low tolerance.

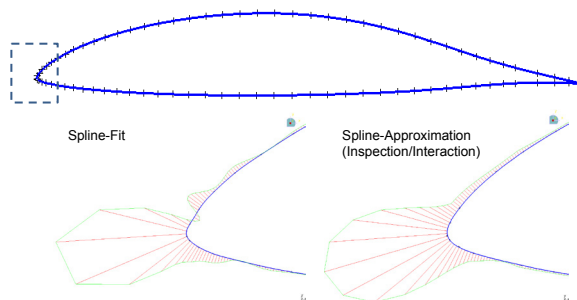


FIGURE 12. Comparison between spline-fit and spline-approximation with porcupine curvature analysis

Due to the described problems when using classical spline-fit curves, which are still popular in aerodynamic design, B-spline curves were used instead. B-spline curves are principally a subset of NURBS-curves and therefore these curves are easy to handle in CAD. Much research has been conducted to efficiently represent existing airfoils with variable and controllable shapes, [11]. However, it was found that in the context of early design, transonic airfoil curves could be reproduced accurately with a low number of control points defining a B-spline curve, as shown in FIGURE 13 for different airfoils. Here the difference between original shape and B-spline representation was below 0.5%, when using 7 control-points for the lower and upper airfoil contour respectively.

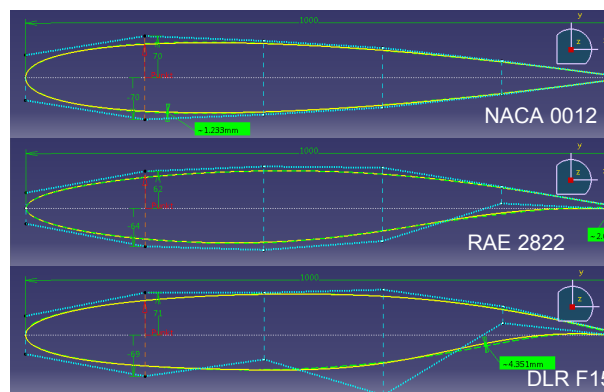


FIGURE 13. Simple B-spline representation of different airfoils with 9 design parameters

	yUp 1 (mm)	yUp 2 (mm)	yUp 3 (mm)	yUp 4 (mm)	yUp 5 (mm)	yLo 2 (mm)	yLo 3 (mm)	yLo 4 (mm)	yLo 5 (mm)
NACA 0012	38	70	62	50	28	-70	-62	-50	-28
RAE 2822	26	62	70	68	36	-64	-70	-55	8
DLR F15	32	71	71	76	48	-69	-41	-101	20

TAB 1. Design parameters of B-spline airfoils

In FIGURE 12 the control points of the B-spline curves of the upper and lower airfoil contour had been connected to start- and endpoints of lines, which are perpendicular and equally-distributed along the chord line of the airfoil. The airfoil shape is finally varied via start- and end-point of each line. To achieve constant curvature around the nose of the airfoil start- and end-point have the same distance. If the trailing edge thickness is always assumed to be constant, the airfoil is defined by 9 design parameters, which are listed in TAB 1 for the examined airfoils, [12].

### 4.2. Nacelle Sections

For the nacelle lines, shown in FIGURE 13, B-splines were utilized in a similar way. However, further geometric properties have to be taken into account, as for example the hi-lite-diameter, droop-angle and other features. Therefore, some of the control points were positioned on lines at a certain relative arc length. This has the advantage that if a characteristic quantity was changed no or only minor changes of the control points are required. This is shown in FIGURE 14, where the hi-lite diameter has been varied, while the relative positions of the control points have remained unchanged.

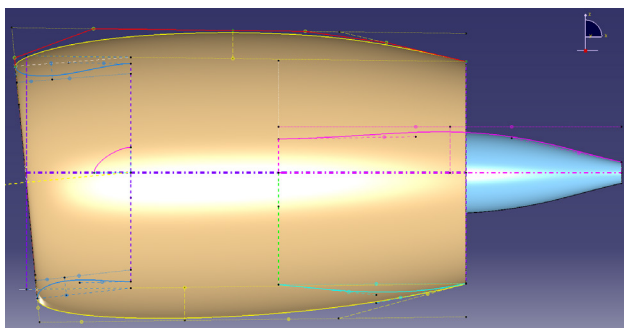


FIGURE 14. CAD geometry of generic single core engine

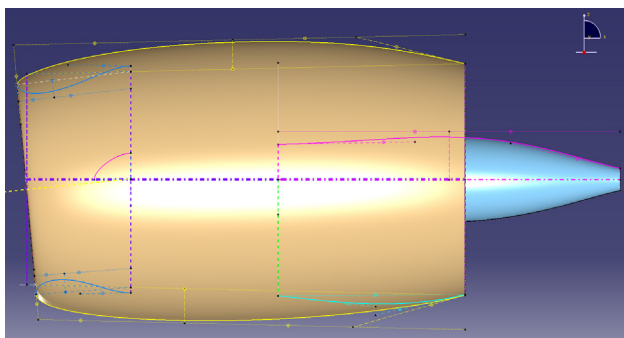


FIGURE 15. CAD geometry of generic single core engine with reduced hi-lite diameter

### 4.3. Fuselage Sections

The prescribed approach of defining control points along lines at relative positions has been applied without any problems for the construction of further aircraft parts. In case of the fuselage sections, the convex hull property of B-spline curves, see [10], is exploited. It affects the shape of a curve segment in a way that the curve stays in a convex hull formed by the corresponding control points. If for example the control points of a fuselage section form a rectangle, the resulting curve will never lie outside of the rectangle. This is demonstrated in FIGURE 16, where the cross section curve is always inside of the convex shaped control point polygons, even if the control points form a rectangle.

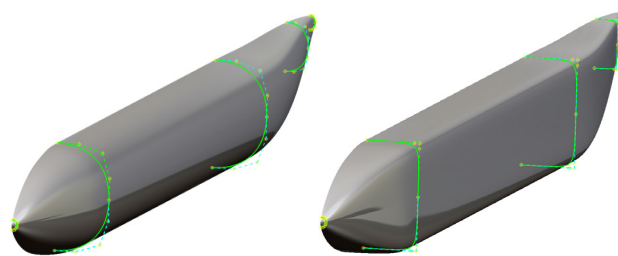


FIGURE 16. Convex hull property of B-splines utilized for fuselage cross-sections

### 4.4. Guide Curves

While section curves are predominantly planar curves with regions of high curvature, the guide curves, which are as important as the section curve for the surface lofting, are in general 3-dimensional curves with less or even no curvature in case of lines. The main problem is that the guide curves must intersect with the section curves. Unfortunately no general strategy for the construction of these curves can be given, but fortunately a huge pallet of functionalities is provided in the generative shape design workbench of CATIA.

In case of the wing, which was shown in FIGURE 6, the leading edge was constructed segment by segment and has in total three trapezoidal parts. While the inner segments have been connected with lines, the outer segment was connected with a bridge-curve, which is tangential to the leading edge line of the mid segment. Then all airfoils were arranged and scaled according to the prescribed twist angles and chord lengths. Next the trailing edge bridge-curves were constructed for the upper and lower airfoil. Due to the use of bridge curves instead of lines, blended winglets or even raked wing tip shapes can be reproduced.

The guide curves used for the lofting of the nacelle are planar and based on circles. The guide curves for the belly fairing are also planar curves and are B-splines curves. The fuselage has an upper and a lower B-spline curve in the symmetry plane. However the construction of the outer fuselage curve, which separates the upper and lower shape, is more elaborate, since it is based on a combination of a planar curve in the x-y-plane and another planar curve in the x-z-plane. A similar approach was used for the loft of the propeller, which was already shown in FIGURE 4. As shown in FIGURE 17, the planform curves have been extruded into the direction of the propeller axis.

Subsequently these surfaces have been intersected with a helical surface, which was modelled based on the prescribed advance ratio of the propeller. The intersection curves are finally used to position and scale the corresponding airfoil sections and secondly they are used as guiding curves for the surface lofting.

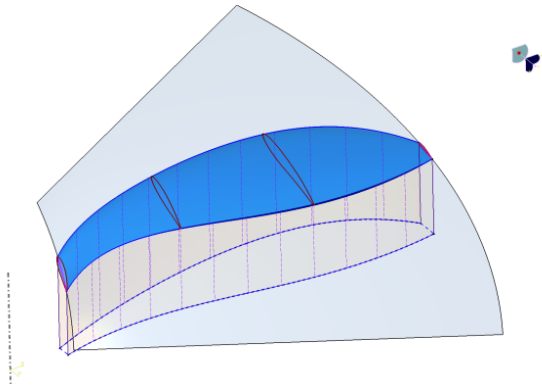


FIGURE 17. Propeller blade from guide curves on helical surface

This approach, which attaches more importance to the guiding curves than to the section curves, has proved to be more advantageous to achieve smooth surfaces. If a loft is generated solely using several section curves, the resulting surface may become wavy in most cases.

**5. ASSOCIATIVE MODELLING**

Since for the generation of single curves or surfaces several construction steps are required, a complete aircraft configuration, which may consist finally of more than 20 surfaces, the construction will become confusing and inscrutable if everything is stored in a single part. Even though there is a structuring available in CATIA for parts, namely sets, which can be used to separate construction sequences adequately, it is more efficient to divide the complete aircraft model into different parts, which are connected via associative links. This is shown in FIGURE 18 for a transport aircraft configuration, which is composed of the parts shown previously. Here, the re-use of parts methodology was used to create a vertical tail plane (VTP) and a horizontal tail plane (HTP). The part, which is re-used, is the wing, but the association to a VTP- and HTP airfoil, has been corrected. Accordingly, the airfoil parts of VTP and HTP have been created from the wing airfoil.

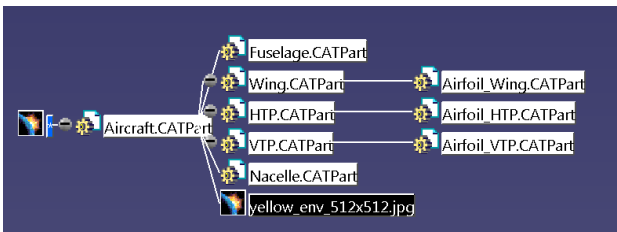


FIGURE 18. Hierarchy of associative aircraft model

The breakdown into several sub-parts enables a concurrent engineering strategy. An engineer, who is responsible for the wing airfoil design has the possibility to test his design either in a 2-dimensional section of an infinite wing or in 3-dimensional environment in which the airfoil is part of a wing loft. The wing in turn may be tested

as an isolated wing or it may be part of the complete aircraft. This hierarchical approach allows a completely new design methodology and is going to replace the traditional component-by-component design process, [13].

In FIGURE 19 aircraft configurations are shown which have been composed of all previously described parts. After positioning of these primary surfaces, secondary surfaces forming wing tips, belly fairing and pylon were generated within the aircraft CAD-model. This ensures that if a position of a primary element is changed, all secondary parts will follow this change. Therefore, if one or more control points have been changed in the airfoil part, as this was already shown in FIGURE 13, this variation is transported via the defined associations from the airfoil part to the wing part and further to the aircraft part. Accordingly the pylon is automatically adapted to the new wing shape.

Since the shapes of the pylon and belly fairing depend primarily on the relative positions of the primary components, the present pylon construction is only applicable for underwing mounted engines. For this reason, the concept of the aircraft is partly fixed. This is also the case for the belly fairing, which was at first designed for a low wing configuration. The configuration, shown in FIGURE 20, has the same components as the configuration shown in FIGURE 19 but with partially changed parameters. While the pylon construction did not cause any problems, the belly fairing did not follow the change from low wing to high wing configuration. It may serve as a sponson for the main landing gear.

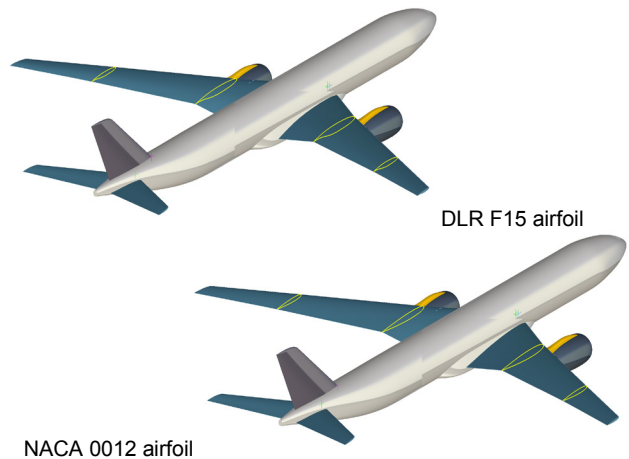


FIGURE 19. Aircraft configurations with different wing airfoil sections

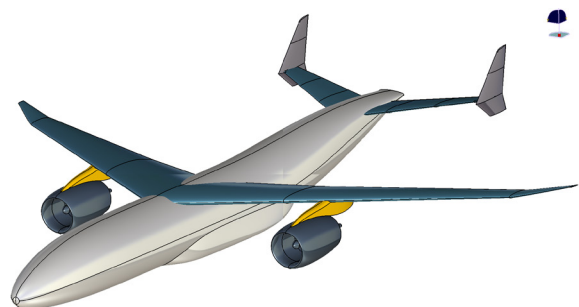


FIGURE 20. High wing transport aircraft configuration with sponson

The aircraft configuration, which is shown in FIGURE 18 or in FIGURE 20 with altered design parameters, is not just yet the final CAD model. In this context it may deal as the master model for virtual testing. For CFD simulations a far field, which represents the outer boundary of the fluid volume, is required and moreover the inner boundary of the fluid volume, which encloses the aircraft has to be watertight. For this purpose an additional CAD-model was constructed, which is associated with all surfaces of the aircraft part, which should be part of the simulation. At first, individual volumes are formed by joining relevant surface panels. Hereafter these volumes are united by Boolean type an operation, which in principle triggers functions to calculate surface/surface intersections and to trim intersection panels. Finally the volume which encloses the aircraft is subtracted from the far field volume, as shown in FIGURE 21. The main advantage in using Boolean operations on volumes is that the result is always a closed volume, which may have cavities.

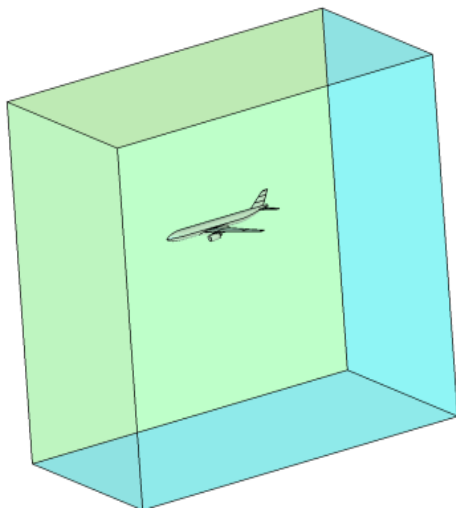


FIGURE 21. CFD fluid volume (reduced far field extension)

This additional CAD-model represents the link to the CFD grid generation and is exported from the CAD system using the native IGES-format.

## 6. DESIGN AUTOMATION

As previously described, design variations can be achieved by changing a parameter value, i.e. the length of a line, in the construction history. This can be done either interactively or in non-interactive mode via so called design tables. These design tables are created at the end of the construction work of a certain part, and are filled with those parameters, which should be varied later. At first the actual values, which are used for the current part are stored in the design table in an excel-file or in an ASCII file format.

A typical design table was already shown in TAB 1. In this case it has 3 rows, where each row contains a certain parameter-combination, which defines the shape of an airfoil. In this case a user can simply switch between parameter configurations to change the airfoil shape. The design tables are associated with corresponding parts of the model hierarchy, in the same way as parts are associated with hierarchically higher parts. A complete

hierarchy including the design tables is shown in FIGURE 22.

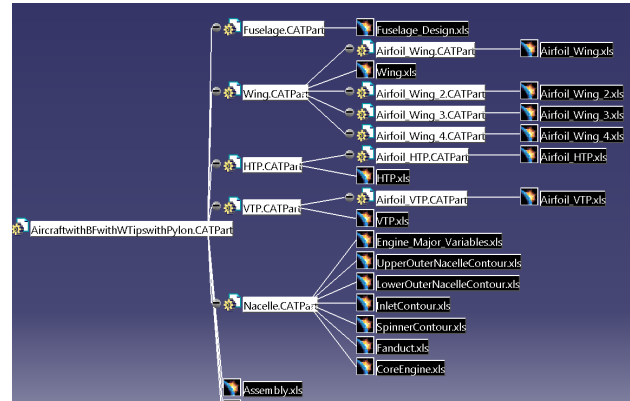


FIGURE 22. Complete hierarchy of associative aircraft model

A design table file can be opened either with an editor or with another application and values can be changed. If the CAD-part, which is associated with a design table, is opened or is already opened, CATIA asks to update the model, if the values in the design table differ from current values used in the model. The same happens, if a part which is lower in the hierarchy has been changed.

This procedure of opening a model and updating it until the final part is up-to-date can be scripted and can be run using a macro in batch mode. If the final part is the CFD-model, the last statement in the macro invokes CATIA to save the geometry in an IGES-format. Finally, the use of design tables and macros allows either non-experienced CAD users to perform design variations or it enables CAD in the loop optimization, as it is described in [3]. In such a loop, the optimizer parses values of variables which should be optimized into the design table and launches CATIA in batch mode with the prescribed macro to update and export the geometry for CFD simulation. At the end of the loop, quantities of the CFD simulation are returned to the optimizer, which prescribes new values of the design variables for the next cycle. This is repeated until an optimum is reached.

For a fully automated design cycle the most critical step is the transition from CAD to grid generation. As already mentioned, a grid generation software was used, which generates hybrid unstructured grids. This software was purchased from CENTAURSoft, [14] and is tailored to CAD-data in IGES or STEP format. In general a more or less intensive manual cleaning of cleaning is required, when the CAD-data are converted into the native geometry representation of the CENTAURSoft grid generator. However, in all cases tested in this study, the CAD-data proved to be very accurate and no manual interaction was necessary. Also the entire grid generation process, where prism layers are generated on all viscous boundaries and tetrahedra are used to fill the remaining fluid volume, has not provided any problems. Parts of a typical volume mesh are shown in FIGURE 23.

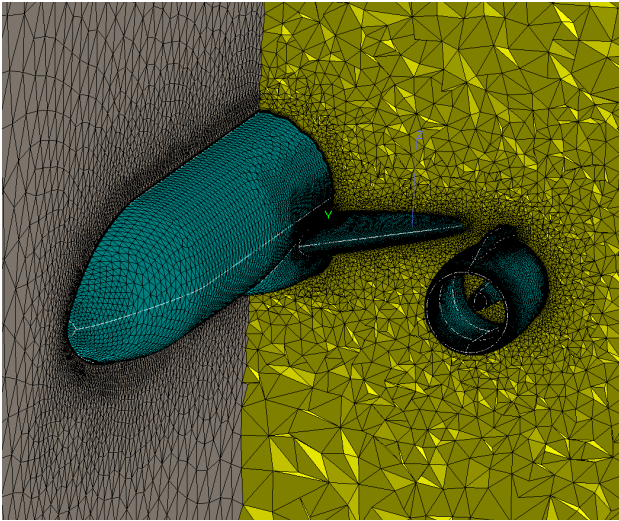


FIGURE 23. Surface mesh and cut through the hybrid volume mesh with prisms and tetrahedrons

To resolve features of the flow, especially along all leading edges and in junction regions the grid density has to be controlled adequately. Fortunately the grid generator from CENTAURSoft has certain capabilities to adapt the density of the mesh to geometric features as for example the local curvature or to the proximity of parts. Due to these properties of CENTAURSoft, the whole grid generation process including CAD cleaning can be run in batch mode and, for the here intended purpose of assessing an aircraft configuration in a very preliminary design phase, settings have been chosen that will lead to moderate grid point numbers.

Finally, for the calculation of the flow solution the DLR flow solver TAU was employed. To achieve extreme short turnaround times all computations have been performed in parallel mode using 144 cores of the DLR C<sup>2</sup>A<sup>2</sup>S<sup>2</sup>E cluster. Furthermore, to save grid point layers near walls also wall function, see [14], were used. This has led to turnaround times of less than 30 minutes for a single configuration. While a CAD model update requires about 1 to 2 minutes and the time for a flow calculation with a satisfying convergence is completed in about 7 minutes, the remainder of the time is required for grid generation.

## 7. EXAMPLES

To demonstrate the possibilities of using parametric CAD in the aerodynamic aircraft design process, a typical transport aircraft configuration as well as some novel aircraft design concepts has been investigated.

In a first example the ability to change the wing airfoil and perform a simulation was demonstrated. The geometry was already shown in FIGURE 19. FIGURE 24 plots the CFD solution for a typical transonic cruise Mach number of 0.82 and an angle of attack of 1°. It should be mentioned that with a conventional CAD process all construction steps from inserting the new airfoils through to the intersection with the pylon would have to be repeated manually.

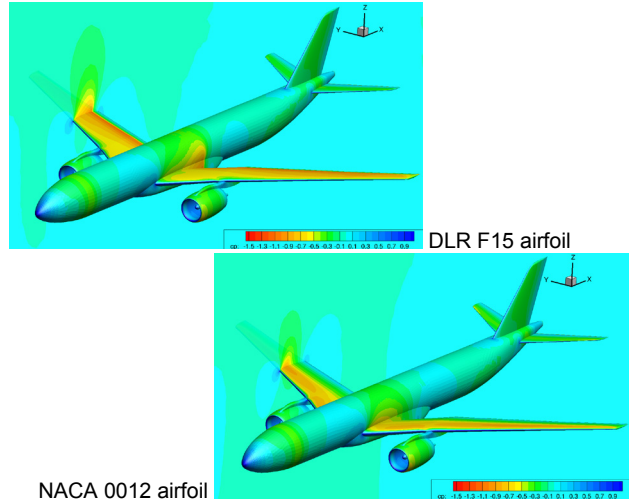


FIGURE 24. Comparison of aircraft with different wing airfoils

Next, a CFD solution for the high wing configuration, which was shown previously in FIGURE 20, is depicted in FIGURE 25. This configuration has some difficult surface intersections, which did not cause any problems in the geometry creation, the grid generation or in the flow calculation.

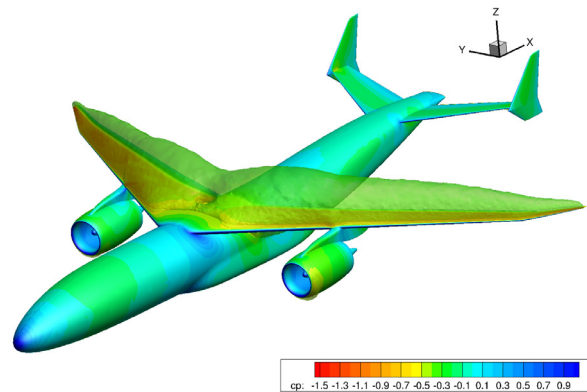


FIGURE 25. CFD solution with iso-Mach=1 surface around high wing aircraft configuration with sponson

At the beginning of this study no secondary parts were available and therefore, nearly no restrictions regarding the positioning of wing and nacelle exist. Since propulsion integration has become a big focus of current research, many novel configurations have their propulsion system mounted above the wing or above the vertical tail plane (VTP) for noise shielding. Therefore, some of these concepts have been studied here with a focus on transonic engine/airframe interference effects. For the configurations shown in FIGURE 26 and FIGURE 27 the nacelle geometry from an under wing mounted engine was adopted. Due to a position in the accelerated flow and due to the more barrel type shape of the nacelles with a maximum thickness in the bottom region, the transonic interference effects are dramatic, despite the fact that the cruise Mach number was relatively low at M=0.78.

A probable improvement can be achieved with more tube-like nacelles with engines having a higher bypass ratio and a position more far away from the upper wing surface.



This is shown in FIGURE 28 and FIGURE 29. The concepts which are presented here are characterized by an oval body shape in the tail region. In combination with the tube-like nacelle shape, this arrangement has a positive effect on the interference.

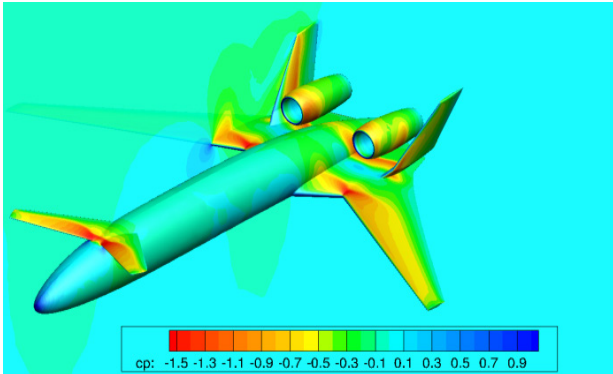


FIGURE 26. Pressure pattern of low noise aircraft concept A

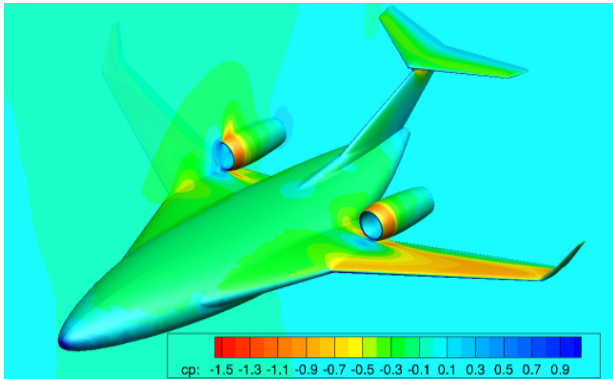


FIGURE 27. Pressure pattern of low noise aircraft concept B

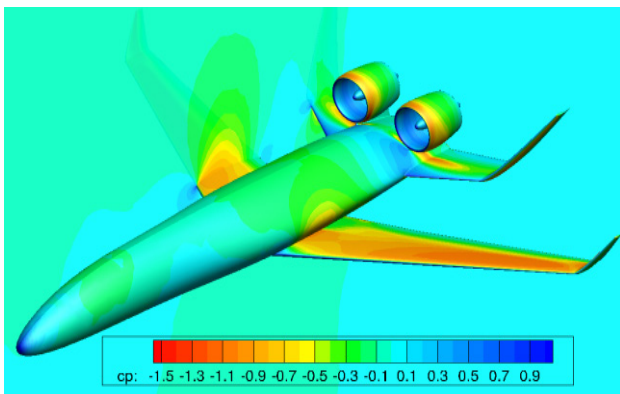


FIGURE 28. low high BPR Low noise aircraft concept A

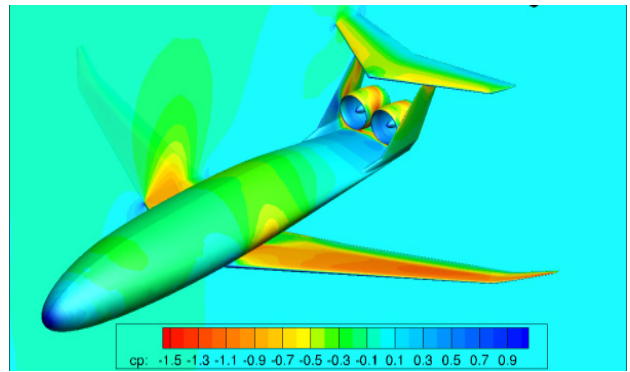


FIGURE 29. Pressure pattern of high BPR Low noise aircraft concept B

In a final example the necessity of secondary parts as for example a belly fairing is demonstrated. In FIGURE 30 a generic business jet configuration is shown where the wing is positioned below the fuselage. This is a common practice in the design of those aircraft, since the structure of the pressurized cabin should not be disrupted by the wing. Despite the fact that no problems occurred when performing a CFD simulation, it turned out that the belly fairing, which has been added afterwards and which is shown in FIGURE 31, led to reduction in drag of about 7.5 percent although the area of the wetted surface was considerably increased.

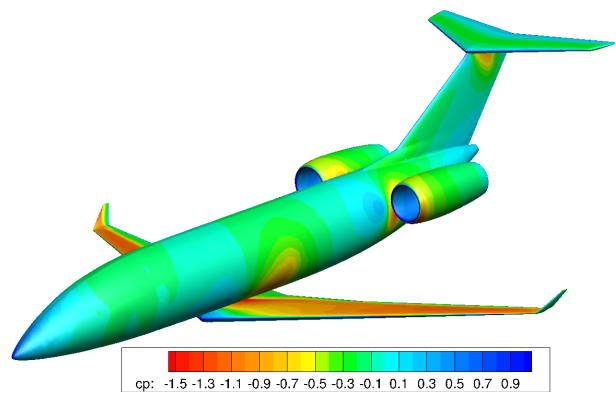


FIGURE 30. Pressure pattern of business jet without belly fairing

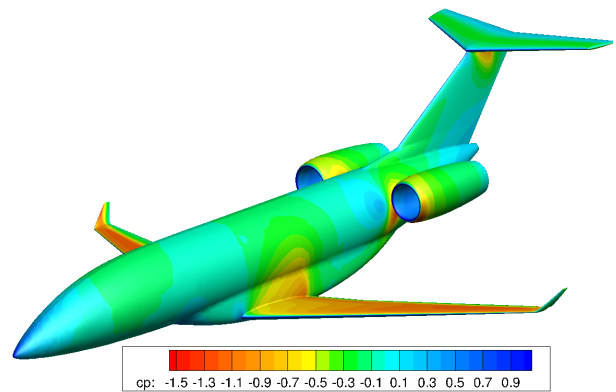


FIGURE 31. Pressure pattern of business jet with belly fairing

## 8. CONCLUSION

The use of the parametric CAD system CATIA in aerodynamic aircraft design has been investigated and demonstrated. It was shown that a parametric CAD system can act as a geometry generator, which produces clean geometry input for CFD simulations. Intersections between surfaces, which are necessary to establish water tightness of the geometry, were calculated without difficulties. However, the major benefit comes from the capability to reuse a construction and to generate variants of a parametric model by replaying the construction sequence, which has been recorded during interactive work. This study showed impressively that for suitable parameter variations a great variety of feasible and realist aircraft configurations could be generated and analyzed. Moderate turnaround times of less than 30 minutes and a sufficient accuracy of the results make this approach also useful early in the aircraft design process. Uncertainties regarding viscous and compressibility effects, can be mitigated to a large degree in early design phases, especially when novel concepts are considered.

The study showed also, that the CAD designer, who constructs a new parametric part, bears a great responsibility to provide flexible and suitable parametric models. In contrast to ordinary CAD systems a careful and foresighted modelling strategy is essential. It was demonstrated that the most successful and efficient strategy was to use the CAD system as it was intended by its developers, to construct a new model interactively. During this it is helpful to test parameter variations from time to time. Due to the possibility to re-use a construction, this additional effort will later be re-paid. In general the concept of re-use of parts or respectively their sequence of construction steps enables also non-CAD experts to make use of parametric CAD design.

To construct a new CAD model practical experience has also shown that it is most convenient to begin with a wireframe of curves and lines. 3-dimensional freeform curves can be created by combining 2-dimensional planar curves. In the end, these curves are used to generate a surface via the loft function, which is the most used function to generate the outer shape of an aircraft. 2-dimensional freeform curves were preferably created from B-splines. This method of curve creation has certain advantages, especially when airfoils or body sections are of interest.

Finally in some examples dealing with conventional and also novel aircraft configurations the prospects of parametric CAD in combination with high fidelity CFD have been illustrated. Since nearly all design variables were associated with design tables and as the simulation chain from grid generation to CFD post-processing runs fully automatically, the step to simulation based aerodynamic design optimization of novel aircraft configuration is self-evident. Especially, when those configurations are assessed and are compared to conventional configurations, which already have converged to an optimal shape, optimizations are indispensable. The future challenge will be to include also other disciplines and to further speed up the turnaround times.

## 9. LITERATURE

[1] Ronzheimer, A. und Rossow, C.-C. und Pflug, M. (1) (1990) Untersuchungen zum Interferenzeinfluss von

modernen Hochbypass-Antriebskonzepten an einer Flügel-Rumpf-Kombination durch Lösung der Euler Gleichung. In: Jahrbuch 1990 der DGLR, Seiten 115-124. DGLR-Jahrestagung 1990, 1.-4. Oktober 1990, Friedrichshafen.

- [2] Galle, M. und Gerhold, T. und Evans, J. (1999) Parallel Computation of Turbulent Flows around Complex Geometries on Hybrid Grids with the DLR-Tau Code. 11th Parallel CFD Conference, Williamsburg (va), 23.-26.05.1999.
- [3] Ronzheimer, Arno und Natterer, Franz Josef und Brezillon, Joël (2010) Aircraft Wing Optimization Using High Fidelity Closely Coupled CFD and CSM Methods. 13th AIAA/ISSMO Multidisciplinary Analysis Optimization Conference, Fort Worth, Texas, Fort Worth, Texas.
- [4] J. A. Samareh: "A Novel Shape Parameterization Approach ", NASA TM-1999-209116, NASA Langley Research Center, Hampton, VA 23681.
- [5] Ronzheimer, A. (2002) Post-Parameterisation of CAD-Geometries Using Freeform Deformation and Grid Generation Techniques. 13. DGLR-Fachsymposium der AG STAB, München (de), 12.-14.11.2002.
- [6] <https://www.3ds.com/products-services/catia/>
- [7] <https://www.ptc.com/>
- [8] <https://www.plm.automation.siemens.com/en/products/nx/>
- [9] Seitz, Arne und Kruse, Martin und Wunderlich, Tobias und Bold, Jens und Heinrich, Lars (2011) The DLR Project LamAir: Design of a NLF Forward Swept Wing for Short and Medium Range Transport Application. 29th AIAA Applied Aerodynamics Conference, 27.-30. Juni 2011, Hawaii, USA.
- [10] Farin, G. (2014), Curves and Surfaces for Computer-Aided Geometric Design: A Practical Guide, Elsevier, ISBN 1483296997, 9781483296999
- [11] Masters, Dominic & J. Taylor, Nigel & Rendall, Thomas & Allen, C & Poole, Daniel. (2015). Review of Aerofoil Parameterisation Methods for Aerodynamic Shape Optimisation. . 10.2514/6.2015-0761.
- [12] J. Wild. Mach and Reynolds Number Dependencies of the Stall Behavior of High-Lift Wing-Sections, Journal of Aircraft, Vol. 50, No. 4 (2013), pp. 1202-1216. <https://doi.org/10.2514/1.C032138>
- [13] J.B. Vos, A. Rizzi, D. Darracq, E.H. Hirschel, Navier-Stokes solvers in European aircraft design, Progress in Aerospace Sciences, Volume 38, Issue 8, 2002, Pages 601-697, ISSN 0376-0421, [http://dx.doi.org/10.1016/S0376-0421\(02\)00050-7](http://dx.doi.org/10.1016/S0376-0421(02)00050-7).
- [14] [www.centaurosoft.com](http://www.centaurosoft.com)
- [15] Knopp, Tobias (2010) Improved Wall Functions Based on the 1D Boundary Layer Equations for Flows with Significant Pressure Gradient. In: New Results in Numerical and Experimental Fluid Mechanics VII Notes on Numerical Fluid Mechanics and Multidisciplinary Design, 112. Springer Verlag, Berlin Heidelberg. Seiten 51-58. ISBN 978-3-642-14242-0. ISSN 1612-2909